Biochimica et Biophysica Acta 818 (1985) 191–199
Elsevier

BBA 72703

Subcellular fractionation of pig coronary artery smooth muscle

A.K. Grover, S.E. Samson and R.M.K.W. Lee

Departments of Neurosciences and Anaesthesia, McMaster University Health Sciences Centre, Hamilton, Ontario L8N 3Z5 (Canada)

(Received February 5th, 1985)

Key words: Ca^{2+} transport; Plasma membrane; Endoplasmic reticulum; Membrane isolation; (Pig smooth muscle)

A detailed procedure for subcellular fractionation of the smooth muscle from pig coronary arteries based on dissection of the proper tissue, homogenization, differential centrifugation and sucrose density gradient centrifugation is described. A number of marker enzymes and Ca^{2+} uptake in presence or absence of oxalate, ruthenium red and azide were studied. The ATP-dependent oxalate-independent azide- or ruthenium red-insensitive Ca^{2+} uptake, and the plasma membrane markers K^+-activated ouabain-sensitive *p*-nitrophenylphosphatase, 5′-nucleotidase and Mg^{2+}-ATPase showed maximum enrichment in the F2 fraction (15–28% sucrose) which was also contaminated with the endoplasmic reticulum marker NADPH: cytochrome *c* reductase, and to a small extent with the inner mitochondrial marker cytochrome *c* reductase, and also showed a small degree of oxalate stimulation of the Ca^{2+} uptake. F3 fraction (28–40% sucrose) was maximally enriched in the ATP- and oxalate-dependent azide-insensitive Ca^{2+} uptake and the endoplasmic reticulum marker NADPH: cytochrome *c* reductase but was heavily contaminated with the plasma membrane and the inner mitochondrial markers. The mitochondrial fraction was enriched in cytochrome *c* oxidase and azide- or ruthenium red-sensitive ATP-dependent Ca^{2+} uptake but was heavily contaminated with other membranes. Electron microscopy showed that F2 contained predominantly smooth surface vesicles and F3 contained smooth surface vesicles, rough endoplasmic reticulum and mitochondria. The ATP-dependent azide-insensitive oxalate-independent and oxalate-stimulated Ca^{2+} uptake comigrated with the plasma membrane and the endoplasmic reticulum markers, respectively, and were preferentially inhibited by digitonin and phosphatidylserine, respectively. This study establishes a basis for studies on receptor distribution and further Ca^{2+} uptake studies to understand the physiology of coronary artery vasodilation.

Introduction

A number of in vivo and in vitro studies have been carried out in recent years to understand coronary vasodilation under physiological and pathophysiological conditions in order to understand the underlying molecular mechanisms [1–5]. Adenosine receptors and adrenergic receptors have been shown to play a key role in this process [2,4,6]. These receptors would presumably be localized in plasma membrane of the smooth muscle cells. Furthermore, as in any other smooth muscle cells, the contractility would be determined by intracellular Ca^{2+} concentration (for review, see Ref. 6) which, in turn, is regulated by binding to, or transport by various cellular membranes as demonstrated by a number of vascular [7–10] and nonvascular smooth muscles [11–18]. Thus it is important to obtain plasma membrane, endo-

Abbreviations: Hepes, 4-(2-hydroxyethyl)-1-piperazineethanesulfonic acid; EGTA, ethylene glycol bis(β-aminoethyl ether)-*N*,*N*′-tetraacetic acid; PMSF, phenylmethylsulfonyl fluoride; TLCK, N^{α}-*p*-tosyl-L-lysine chloromethyl ketone.

plasmic reticulum and mitochondrial membrane enriched fractions in order to understand the molecular mechanisms responsible for vasodilation of the coronary arteries. Some studies using microsomal fractions prepared from coronary arteries [4,19,20] have been previously reported. In this study we present a detailed procedure on dissection of porcine coronary artery to obtain relatively pure smooth muscle and a subcellular fractionation procedure which yields a fraction enriched in plasma membrane and also others enriched slightly in the endoplasmic reticulum or the mitochondrial membranes. ATP-dependent Ca^{2+}-uptake properties of the subcellular fractions are also reported.

Experimental methods

Tissue dissection. Typically 40 pig hearts were placed on ice, and tissue slices containing the right coronary artery were cut from each [19] and placed in ice-cold Hepes-Krebs solution containing 116 mM NaCl, 4.6 mM KCl, 1.2 mM $MgSO_4$, 1.2 mM NaH_2PO_4, 2.5 mM $CaCl_2$, 11 mM glucose and 11 mM Hepes (pH 7.2). The slices were mounted on stainless steel probes [19], cutting off the cardiac tissue and the fat, and were then inverted and placed in the ice-cold preparation solution (250 mM sucrose, 1 mM dithiothreitol and 0.5% of an ethanolic solution containing 100 mM PMSF). Light and electron microscopy of the inverted arteries showed that the vessels had already lost the endothelium during processing and that these contained a large amount of media layer characteristic of a muscular artery, and an adventitia layer and occasional nerves. No cardiocytes or erythrocytes were observed. The inverted artery was mounted on the probe again to dissect out the media layer which was subsequently placed in the ice-cold preparation solution. The media layer so removed was observed to contain predominantly smooth muscle cells, some collagen and occasional patches of elastin. Thus, this tissue used for the subsequent subcellular fractionation was devoid of endothelial layer, adventitia, erythrocytes, cardiocytes and nerve cells.

Subcellular fractionation. Routinely, 3–4 g tissue was minced and suspended in 20 volumes of the preparation solution and homogenized using a Polytron PT 20 for four times 5 s at 0°C. Subsequent procedure is given in Scheme I. Variations of this and other homogenization procedures were used in the initial stages as described in Results.

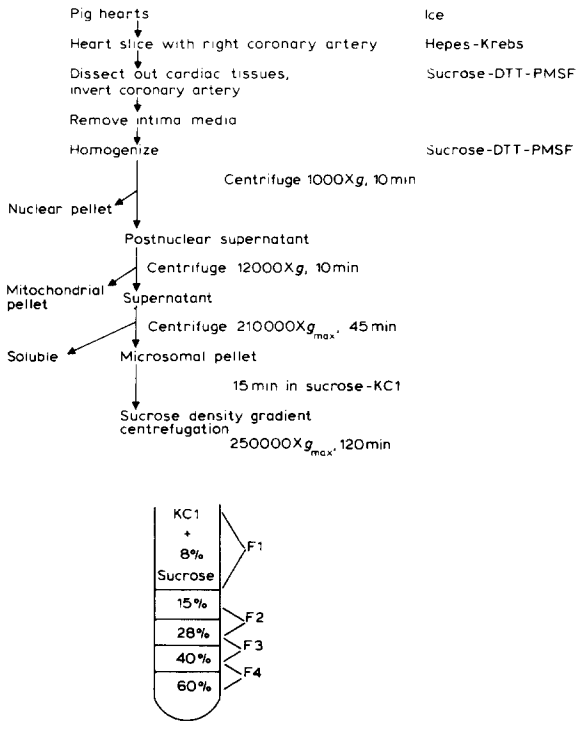

Scheme I. Subcellular fractionation. DTT, dithiothreitol.

Enzyme assays. K^+-activated ouabain-sensitive *p*-nitrophenylphosphatase, ouabain-insensitive *p*-nitrophenylphosphatase, 5′-nucleotidase, Mg^{2+}-ATPase, cytochrome *c* oxidase, NADPH : cytochrome *c* reductase, rotenone-insensitive NADH:cytochrome *c* reductase, phosphodiesterase I and alkaline phosphatase were carried out at 37°C as described previously [8,11,14,15].

Ca^{2+} uptake. The ATP-dependent Ca^{2+} uptake was carried out under the reaction conditions described by Wuytack et al. [19]. Routinely, only the azide-insensitive Ca^{2+} uptake in the absence of oxalate was carried out. The reaction mixture contained 30 mM imidazole-HCl (pH 6.8) (37°C), 100 mM KCl, 5 mM $MgCl_2$, 5 mM ATP, 1 mM EGTA, 5 mM sodium azide, 0.85 mM $CaCl_2$, trace amounts of $^{45}CaCl_2$, and 20–100 μg protein sample of the subcellular fraction. After 20 min at 37°C the reaction mixture was filtered through 0.45 μm nitrocellulose (Millipore) filters and the

filters were washed twice with a solution containing 250 mM sucrose, 40 mM imidazole-HCl (pH 7.0) and 0.5 mM EGTA. The radioactivity on the filters was determined by scintillation counting. Concomitantly, blanks without any membranes were also run. The ATP-dependent Ca^{2+} uptake was then defined as the Ca^{2+} uptake in presence of ATP minus the uptake in absence of ATP. Sodium azide, ruthenium red or oxalate were added in the various experiments only as described in Results. For experiments involving digitonin and phosphatidylserine the membranes were premixed with required concentrations of these agents at 0°C and then added to the Ca^{2+} uptake media. This resulted in a 2.6-fold dilution and only the concentrations after the dilution are shown in Results.

Microscopy. Light microscopy of the tissues and electron microscopy of the tissues or the membrane pellets were carried out as described previously [9,10].

Statistical analysis. Correlation studies employed linear correlation coefficient determination. All other statistics were carried out by using unpaired two-tailed Student's *t*-test.

Results

Establishment of subcellular fractionation methods

In initial experiments tissue homogenization was carried out by using a motor-driven Teflon pestle in a glass tube. However, very low yields of the cell-free extracts were obtained. Subsequently, the tissues were homogenized using Polytron PT-20 for different time periods to determine optimal conditions for maximum ratio of the plasma membrane marker 5′-nucleotidase to the inner mitochondrial marker cytochrome *c* oxidase in the microsomes, as well as maximum yield. Based on these preliminary experiments, the protocol for preparation of microsomes given in Scheme I was devised. The microsomes so obtained, however, aggregated. Subsequently, it was observed that washing the microsomes with a solution containing KCl resulted in removal of a large amount of soluble proteins and gave microsomes which did not aggregate as readily. In another set of initial experiments, the tissues were homogenized in the presence or absence of the protease inhibitors PMSF, TLCK and soybean trypsin inhibitor, and

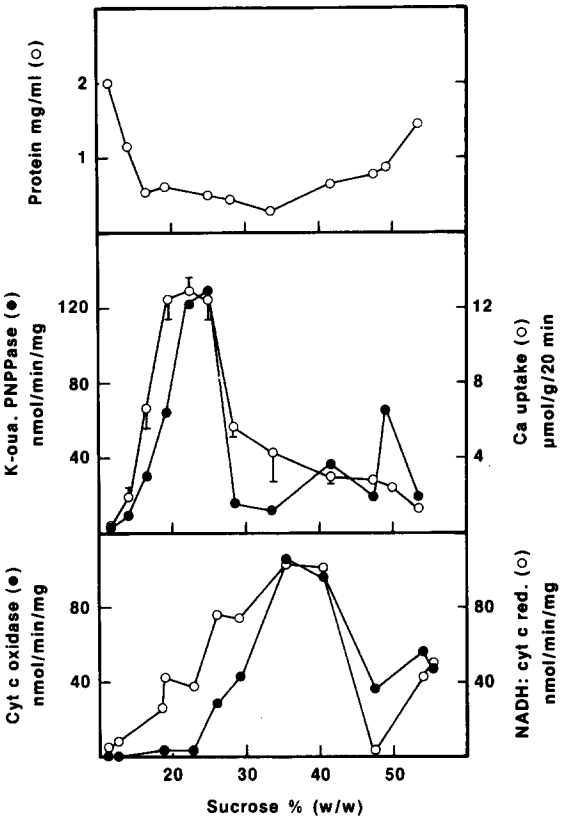

Fig. 1. Continuous sucrose density gradient centrifugation. Microsomes were suspended in 250 mM sucrose, and adjusted to 250 mM sucrose and 700 mM KCl and incubated for 15 min at 0°C, and then centrifuged at 250000 × g_{max} for 120 min on continuous sucrose density gradients (8% to 60%). Fractions were collected from the top and sucrose concentrations determined by refractometry. K-oua. PNPPase, K^+-activated ouabain-sensitive *p*-nitrophenylphosphatase; Cyt *c* oxidase, cytochrome *c* oxidase; NADH : cyt *c* red., rotenone-insensitive NADH : cytochrome *c* reductase. The values are means ± S.E. of 3–6 replicates.

the resulting post-nuclear supernatant assayed for ATP-dependent azide-insensitive Ca^{2+}-uptake, 5′-nucleotidase, cytochrome *c* reductase and rotenone-insensitive NADH : cytochrome *c* reductase. None of these activities were significantly affected. Therefore, in all the subsequent experiments the preparation buffer containing PMSF as used by Wuytack et al. [19,20] was employed.

The microsomes (not washed in KCl) suspended in 250 mM sucrose were mixed with a solution to obtain 250 mM sucrose and 700 mM

TABLE I

SPECIFIC ACTIVITIES OF ENZYME ACTIVITIES AND Ca^{2+} UPTAKE IN SUBCELLULAR FRACTIONS

The enzyme activities are expressed as means ± S.E. of 3–6 preparations, units: nmol/min per mg. For Ca^{2+} uptake in each instance only a representative experiment is shown and the values are means ± S.E. of six replicates.

	Postnuclear supernatant	Mitochondrial
K^+-ouabain-sensitive *p*-nitrophenylphosphatase	11.5 ± 3.6	17.3 ± 5.4
Ouabain-insensitive *p*-nitrophenylphosphatase	131.8 ± 8.8	79.1 ± 5.3
5′-Nucleotidase	4.2 ± 1.8	10.1 ± 2.1
Mg^{2+}-ATPase	60	42
Cytochrome *c* oxidase	23.9 ± 8.1	294.0 ± 81.3
NADH : cyt *c* reductase (rotenone insensitive)	21.9 ± 3.9	85.4 ± 17.4
NADPH : cyt *c* reductase	1.1 ± 0.5	2.2 ± 0.1
ATP-dependent Ca^{2+} uptake		
No oxalate		
Azide inhibition (%)	73.6 ± 5.5	89.9 ± 2.1
Ruthenium red inhibition (%)	75.5 ± 3.6	87.5 ± 6.2
Azide-insensitive (no oxalate) (nmol/20 min per mg)	1.3 ± 0.1	3.8 ± 1.7
Azide-insensitive oxalate-stimulated (nmol/20 min per mg)	8.3 ± 0.3	1.5 ± 2.7

KCl, and centrifuged on a continuous sucrose density gradient. Fractions were collected and assayed for sucrose concentration, protein concentration, the plasma membrane marker K^+-activated ouabain-sensitive *p*-nitrophenylphosphatase, the inner mitochondrial marker cytochrome *c* oxidase and for rotenone-insensitive NADH : cytochrome *c* reductase, and for the Ca^{2+} uptake in presence of ATP and sodium azide. As expected from the inital KCl wash experiments, a large amount of protein was observed in the top fractions (Fig. 1). The Ca^{2+} uptake and the plasma membrane marker showed a similar migration with their highest specific activities at 15 to 25% sucrose. Cytochrome *c* oxidase and the rotenone insensitive NADH-dependent cytochrome *c* reductase, however, showed broader distribution with their highest specific activities at 35 to 45% sucrose. Based on this information obtained in three experiments, the protocol in Scheme I was devised to fractionate KCl-treated microsomes on discontinuous gradients. Thus the protocol in Scheme I is based on the initial experiments on homogenization, information that KCl wash removes soluble proteins from microsomes and the sucrose density pattern of the various marker activities.

Distribution of biochemical activities in subcellular fractions

Table I shows the distribution of a number of biochemical activities in the various subcellular fractions (see Scheme I). The points to note are: (a) F2 was maximally enriched in the plasma membrane marker K^+-activated ouabain-sensitive *p*-nitrophenylphosphatase but not as much in the ouabain-insensitive *p*-nitrophenylphosphatase; (b) the distribution of 5′-nucleotidase and Mg^{2+}-ATPase paralleled that of K^+-activated ouabain-sensitive *p*-nitrophenylphosphatase except for the soluble fraction which contained substantial amounts of 5′-nucleotidase but very little of the K^+-activated ouabain-sensitive *p*-nitrophenylphosphatase; (c) both, the putative endoplasmic reticulum markers NADPH : cytochrome *c* reductase [15] and the rotenone insensitive NADH : cytochrome *c* reductase [16,18] showed similar distribution with maximal enrichment in F3; (d) the inner mitochondrial marker cytochrome *c* oxidase was maximally enriched in the mitochondrial and the F3 fractions; and (e) sodium azide and ruthenium red showed pronounced inhibition of the ATP-dependent Ca^{2+} uptake by the postnuclear supernatant and the mitochondrial fractions but not of

Soluble	Microsomal	F1	F2	F3	F4
–	46.0±14.4	9.2±2.9	196.7±61.6	100.1± 31.3	27.6± 8.6
118.6±7.9	290.0±19.4	21.1±1.4	329.5±22.0	342.7± 22.9	171.3±11.4
3.4±0.8	9.2± 1.3	5.5±2.1	31.9± 2.1	13.4± 2.1	5.0± 0.2
6.0	120	42	408	264	84
0	64.5±19.1	0.2±0.2	50.2±21.5	337.0±121.9	109.9±23.9
4.4±0.9	102.9±17.5	13.1±4.4	157.7±61.3	280.3± 48.2	56.9±26.3
0.1±0.1	6.1± 0.8	1.3±0.3	9.8± 1.9	17.9± 3.2	6.4± 1.2
–	16.4± 7.3	–	−13.6±10.8	9.8± 8.3	21.0± 8.7
–	27.6± 3.0	–	−4.9± 4.3	1.0± 8.4	41.9± 7.2
0.3±0.3	6.5± 2.3	1.2±0.9	16.8± 3.6	6.0± 2.2	1.8± 0.3
–	10.5± 1.2	–	10.9± 1.6	44.6± 4.5	9.8± 2.2

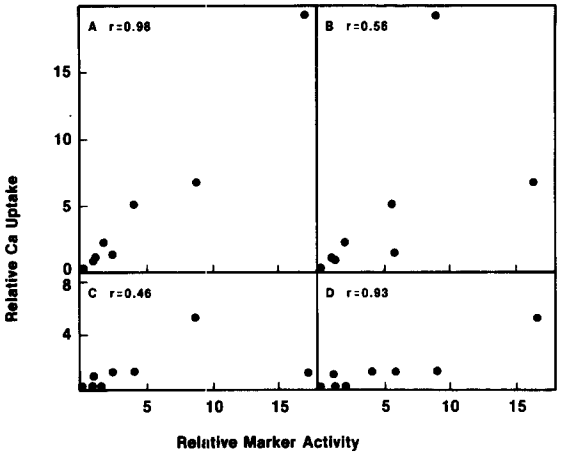

Fig. 2. Correlation plots for azide insensitive ATP-dependent Ca^{2+} uptake and markers. Relative activity = (specific activity of an enzyme or uptake in a given fraction)/(specific activity of the same in the postnuclear supernatant fraction). (A) Oxalate-independent Ca^{2+} uptake vs. K^+-activated ouabain-sensitive *p*-nitrophenylphosphatase. (B) Oxalate-independent Ca^{2+} uptake vs. NADPH : cytochrome *c* reductase. (C) Oxalate-stimulated Ca^{2+} uptake vs. K^+-activated ouabain-sensitive *p*-nitrophenylphosphatase. (D) Oxalate-stimulated Ca^{2+} uptake vs. NADPH : cytochrome *c* reductase. $P < 0.05$ for $r > 0.71$.

the uptake by the microsomal, F1, F2, F3 or F4 fractions, (f) the ATP-dependent azide-insensitive Ca^{2+} uptake showed a distribution parallel to the plasma membrane markers, and (g) oxalate-stimulated the ATP-dependent azide-insensitive Ca^{2+} uptake maximally in the F3 fraction (Table I). The data on the Ca^{2+} uptake were analysed for correlation with the membrane markers (Fig. 2). The azide-insensitive oxalate-independent Ca^{2+} uptake correlated extremely well with the plasma membrane marker K^+-activated ouabain insensitive *p*-nitrophenylphosphatase but not with the putative endoplasmic reticulum marker NADPH : cytochrome *c* reductase (Fig. 2A and B). The oxalate-stimulated Ca^{2+} uptake, however, showed a good correlation with the endoplasmic reticulum (Fig. 2D) and not with the plasma membrane marker (Fig. 2C).

Tables II and III give the recovery data on protein and the various biochemical activities, respectively. Two major conclusions emerge from Table II: (a) protein yields were nearly quantitative in all the steps, and (b) the overall yields of the plasma membrane enriched fraction F2 and the endoplasmic reticulum enriched fraction F3 were 1.2 mg and 0.9 mg/g tissue, respectively.

TABLE II

PROTEIN RECOVERY IN SUBCELLULAR FRACTIONS

The values presented are means ± S.E. of four preparations.

	mg/g tissue	% postnuclear supernatant
Postnuclear supernatant	54.8 ± 4.8	–
Mitochondrial	3.0 ± 0.3	5.5 ± 0.5
Soluble	39.5 ± 7.0	72.1 ± 12.8
Microsomal	11.8 ± 1.4	21.5 ± 2.6
		Total 99.1
	mg/mg tissue	% microsomal
F1	5.6 ± 0.4	47.5 ± 3.4
F2	1.2 ± 0.2	10.2 ± 1.7
F3	0.9 ± 0.2	7.6 ± 1.7
F4	1.8 ± 0.5	15.3 ± 4.2
		Total 80.6

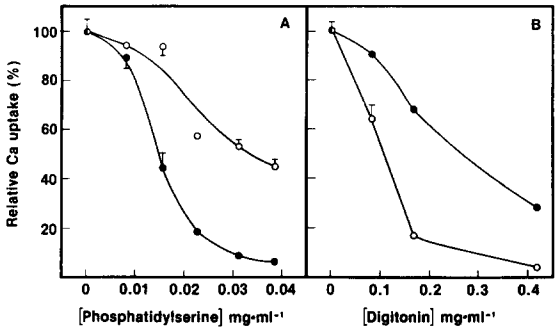

Fig. 3. Effect of phosphatidylserine and digitonin on the oxalate-independent Ca^{2+} uptake by the pig coronary artery F2 fraction (○) and the oxalate-stimulated Ca^{2+} uptake by the F3 fraction (●). The points are means ± S.E. of 6–9 replicates.

Table III shows that the overall recovery of the various biochemical markers was nearly quantitative in most instances except for Ca^{2+} uptake. Once again, it is noted that whereas the K^+-activated ouabain-sensitive *p*-nitrophenylphosphatase was virtually undetectable in the soluble fraction 44% of the total 5′-nucleotidase was present in this fraction. This is consistent with distribution of 5′-nucleotidase reported from a number of smooth muscles (for review, see Ref. 6). The lack of parallelism between the distribution of the ouabain-sensitive and the ouabain-insensitive *p*-nitrophenylphosphatase is also obvious from Table III. The overall yield of the ATP-dependent azide-insenstive oxalate-independent Ca^{2+} uptake was 59% in contrast to the overall yield for the oxalate-stimulated Ca^{2+} uptake which was only

TABLE III

RECOVERY OF ENZYME ACTIVITIES

The values are mean ± S.E. of % yield from 3–6 preparations, except for Mg^{2+}-ATPase which represents only one preparation. K-oua. PNPPase, K^+-activated ouabain-sensitive *p*-nitrophenylphosphatase; oua-ins. PNPPase, ouabain-insensitive *p*-nitrophenylphosphatase; NADH : cyt red, NADH-dependent cytochrome *c* reductase; cyt oxidase, cytochrome *c* oxidase; Ca^{2+} uptake, ATP-dependent azide-insensitive Ca^{2+} uptake.

	% Postnuclear supernatant			% Microsomal			
	Mitochondrial	Soluble	Microsomal	F1	F2	F3	F4
K-oua. PNPPase	7.0 ± 1.8	–	87.2 ± 29.3	9.7 ± 2.4	48.5 ± 15.0	20.6 ± 7.9	9.4 ± 6.3
Oua-ins. PNPPase	3.3 ± 0.6	58.3 ± 9.4	24.0 ± 6.2	8.4 ± 2.8	24.2 ± 5.8	22.1 ± 9.1	19.6 ± 5.9
5′-Nucleotidase	10.4 ± 0.8	44.0 ± 4.3	50.0 ± 14.3	19.5 ± 8.9	23.2 ± 6.1	10.2 ± 3.1	7.3 ± 2.7
Mg^{2+}-ATPase	2.5	12.2	43.2	16.8	46.1	15.6	10.7
NADH : cyt red	20.4 ± 1.6	13.2 ± 4.0	111.3 ± 23.1	8.2 ± 4.0	14.4 ± 3.3	26.3 ± 11.5	13.3 ± 6.3
NADPH : cyt red	10.6 ± 2.2	6.3 ± 6.3	80.3 ± 7.7	11.6 ± 3.7	21.0 ± 5.9	29.4 ± 8.2	27.9 ± 8.7
Cyt oxidase	70.3 ± 27.1	–	68.0 ± 34.3	0.3 ± 0.3	8.2 ± 2.7	41.8 ± 10.7	28.9 ± 7.5
Oxalate-independent Ca^{2+} uptake	13.3 ± 7.2	–	95.4 ± 19.7	–	44.9 ± 7.2	11.5 ± 4.1	4.6 ± 0.8
Oxalate-stimulated Ca^{2+}-uptake	5.7 ± 2.3	–	20.1 ± 2.3	–	12.4 ± 1.9	49.4 ± 5.0	24.4 ± 5.6

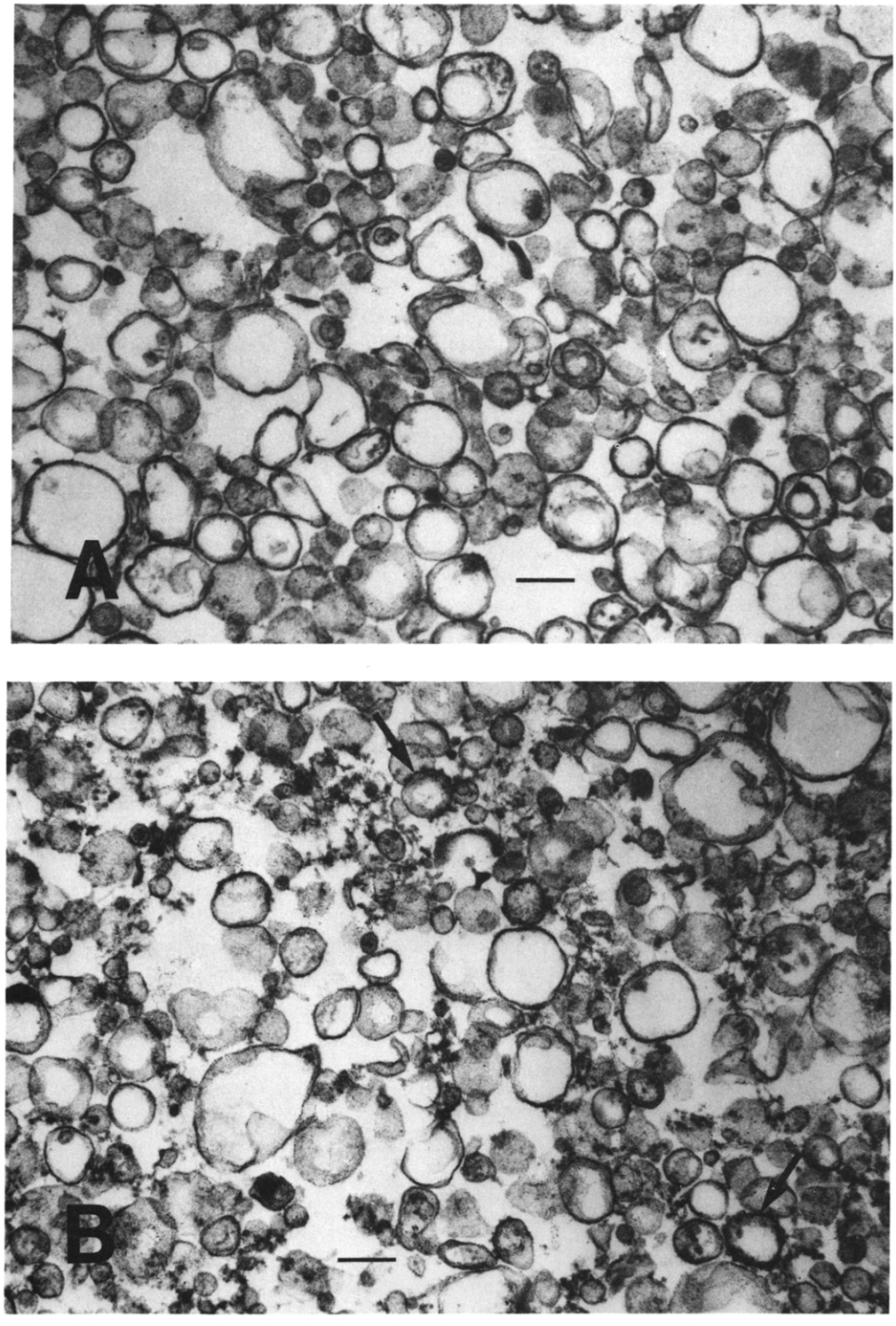

Fig. 4. Electron micrograph of subcellular fractions F2 (A) and F3 (B)from pig coronary arteries. Note the presence of intact, smooth-surfaced membrane vesicles in the F2 fraction and the presence of rough-surfaced membrane vesicles (arrows) in the F3 fractions. Bar = 300 nm.

18%. This is consistent with our previous findings that the oxalate-stimulated Ca^{2+} uptake in smooth muscles diminished preferentially during the membrane purification [21].

Effect of digitonin and phosphatidylserine on Ca^{2+} uptake

The ATP-dependent azide-insensitive Ca^{2+} uptake was examined. The fraction F2 was used for the oxalate-independent Ca^{2+} uptake and F3 for the oxalate-stimulated Ca^{2+} uptake. Digitonin preferentially inhibited the oxalate-independent Ca^{2+} uptake. Digitonin preferentially inhibited the oxalate-independent Ca^{2+} uptake and phosphatidylserine preferentially inhibited the oxalate-stimulated Ca^{2+} uptake (Fig. 3).

Electron microscopy on subcellular fractions

The membrane fractions mitochondrial, F2, F3 and F4 were examined although Fig. 4 shows only the two fractions, F2 and F3. The mitochondrial fraction contained condensed mitochondria, some nuclei, ribosomes, rough endoplasmic reticulum and some collagen fibers. The fraction F4 again contained some vesicles, ribosomes, collagen fragments and mitochondria. The fraction F2 contained predominantly smooth surface vesicles 50–400 nm in diameter, and some ribosomes (Fig. 4A). The fraction F3 contained smooth surface vesicles, rough endoplasmic reticulum ribosomes and mitochondria (Fig. 4B).

Discussion

The results have been presented on distribution of biochemical activities, Ca^{2+} uptake and electron microscopy of the subcellular fractions from the smooth muscle layer of pig large coronary artery. These will be discussed here further in terms of validity of the markers used, membrane contents of F2, F3 and the mitochondrial fractions, discrepancies in the correlation data and importance of this preparation.

K^+-activated ouabain-sensitive *p*-nitrophenylphosphatase has been shown to be a valid plasma membrane marker in smooth muscle (for review, see Ref. 6) since it represents a partial reaction of the Na^+ pump as demonstrated in rat myometrium [1,22]. 5′-Nucleotidase and Mg^{2+}-ATPase have also been previously employed as plasma membrane markers, although 5′-nucleotidase is known to occur in the soluble fraction in large amounts and Mg^{2+}-ATPase may also originate from desensitized myosin present in the fractions (for review, see Ref. 6). The distribution obtained for these two plasma membrane markers was consistent with these observations. NADPH : cytochrome *c* reductase has been used as an endoplasmic reticulum marker in smooth muscle (Refs. 15 and 6 (review)). Rotenone-insensitive NADH : cytochrome *c* reductase, however, has been used as a marker for outer mitochondrial membrane or for endoplasmic reticulum [15,16,18]. In this study the two reductase activities, however, paralleled. Thus it is unclear whether the outer mitochondrial membrane co-travelled with the endoplasmic reticulum or not. Some of the markers studied here (e.g., K^+-activated ouabain-sensitive *p*-nitrophenylphosphatase) may also depend on the membrane sidedness. Therefore, a precaution was taken to carry out the assays under hypotonic shock conditions which are known to expose both the membrane surfaces (Ref. 6, review).

The oxalate-stimulated azide-insensitive Ca^{2+} uptake correlated extremely well with the putative endoplasmic reticulum marker but not with the plasma membrane marker. The Ca^{2+} uptake distribution, however, in the absence of oxalate paralleled the plasma membrane marker distribution. These data are consistent with the previous observations that the oxalate-independent azide-insensitive Ca^{2+} uptake is localized in the plasma membrane [8–12,13–17,19,21] but the oxalate-stimulated Ca^{2+} uptake may reside in the endoplasmic reticulum [16,18] or another subfraction of plasma membrane [13]. The localization of the oxalate-stimulated Ca^{2+} uptake in the endoplasmic reticulum, is, however, strengthened by the differential effects of digitonin and phosphatidylserine on the two modes of Ca^{2+} uptake in this study and as previously reported in the literature [21]. The problem of relatively lower yield of the oxalate-stimulated Ca^{2+} uptake reported earlier in rat myometrium [21] persisted here as well. It is interesting to note that if the overall yield of the oxalate-stimulated Ca^{2+} uptake (18%) were to be comparable to that of the oxalate independent uptake (59%), a level of 146 μmol/g per 20 min or

an enrichment of 18-fold over postnuclear supernatant would be expected in the F3 fraction, instead of the 5-fold enrichment observed.

The data presented here, the uncertainties in the markers discussed above, the lack of reliable markers in smooth muscle for lysosomal and myofibrillar markers and the low yield of the oxalate-stimulated Ca^{2+} uptake clearly demonstrate the difficulties in numerical determination of the membrane purity. An attempt was made to calculate membrane contents of the various fractions using a method modified from Matlib et al. [15]. The computation showed that F2 contained 72% plasma membrane, 23% endoplasmic reticulum and 5% mitochondrial membranes; and F3 consisted of 39% endoplasmic reticulum 30% plasma membrane 26% mitochondrial and 5% other protein. The microsomal fraction contained 22% plasma membrane, 15% endoplasmic reticulum, 13% mitochondrial and 50% other proteins, and the mitochondrial fraction contained 8% plasma membrane, 12% endoplasmic reticulum, 22% mitochondrial and 58% other proteins. Thus, the electron microscopy and the biochemical marker data are all consistent with the F2 fraction being predominantly plasma membrane with a moderate level of contamination of endoplasmic reticulum and very low mitochondrial contamination. The fraction F3 which is maximally enriched in endoplasmic reticulum, is contaminated with plasma membrane as well as with the inner mitochondrial membrane but may serve as a useful tool for studying the properties of the oxalate-stimulated Ca^{2+} uptake or for further purification of the membranes capable of such an uptake. The puzzling low level of the ruthenium red- or azide-insensitive Ca^{2+} uptake in the F3 fraction despite the high specific activity of cytochrome *c* oxidase may result from further damaging of the mitochondria during the purification process. The mitochondrial fraction again contains several impurities and hence may be useful only for further purification of mitochondria or for studying Ca^{2+} uptake using azide and ruthenium red as controls. Thus, this procedure provides us with methods for studying the distribution of receptors in the coronary artery, for studying the effects of pH, adenosine and other factors and the Ca^{2+} handling properties of plasma membrane, endoplasmic reticulum and mitochondria but using proper controls.

Acknowledgments

The authors acknowledge Drs. F. Wuytack and R. Casteels of K.U.L. Campus Gasthuisberg, Leuven, Belgium, for demonstrating their dissection and other procedures, and various colleagues for their reading the manuscript. This work was supported by Heart and Stroke Foundation of Ontario and R.M.K.W.L. is a Career Scientist supported by Ontario Ministry of Health.

References

1 Downing, S.E., Lee, J.C. and Weinstein, E.M. (1982) Am. J. Physiol. 243, H252–H258
2 Fenton, R.A., Rubio, R. and Berne, R.M. (1981) J. Appl. Physiol. 51, 179–184
3 Gwirtz, P.A. and Stone, H.L. (1982) Am. J. Physiol. 243, H13–H19
4 Mustafa, S.J. (1980) Mol. Cell. Biochem. 31, 67–87
5 Rooke, T.W. and Sparks, H.V., Jr. (1981) Experientia 37, 982–983
6 Daniel, E.E., Grover, A.K. and Kwan, C.Y. (1983) Calcium, in Handbook of Smooth Muscle (Stephens, N.L., ed.), pp. 1–88, CRC Press, Boca Raton
7 Kutsky, P. and Weiss, G.B. (1982) Blood Vessels 19, 53–64
8 Kwan, C.Y., Garfield, R.E. and Daniel, E.E. (1979) J. Mol. Cell. Cardiol. 11, 639–659
9 Kwan, C.Y., Triggle, C.R., Grover, A.K., Lee, R.M.K.W. and Daniel, E.E. (1984) Prep. Biochem. 13, 275–314
10 Kwan, C.Y., Triggle, C.R., Grover, A.K., Lee, R.M.K.W. and Daniel, E.E. (1984) J. Mol. Cell. Cardiol. 16, 747–764
11 Grover, A.K., Kannan, M.S. and Daniel, E.E. (1980) Cell Calcium 1, 135–146
12 Grover, A.K., Kwan, C.Y., Garfield, R.E., McLean, J., Fox, J.E.T. and Daniel, E.E. (1980) Can. J. Physiol. Pharmacol. 58, 1102–1113
13 Grover, A.K. and Kwan, C.Y. (1984) Arch. Int. Pharmacodyn. Ther. 267, 4–12
14 Kwan, C.Y., Lee, R.M.K.W. and Grover, A.K. (1983) Mol. Physiol. 3, 53–69
15 Matlib, M.A., Crankshaw, J., Garfield, R.E., Crankshaw, D.J., Kwan, C.Y., Branda, L.A. and Daniel, E.E. (1979) J. Biol. Chem. 254, 1834–1840
16 Raeymaekers, L., Wuytack, F., Eggermont, J., Deschutter, G. and Casteels, R. (1983) Biochem. J. 210, 315–322
17 Sakai, Y., McLean, J., Grover, A.K., Garfield, R.E., Fox, J.E.T. and Daniel, E.E. (1981) Can. J. Physiol. Pharmacol. 59, 1260–1267
18 Wibo, M., Morel, N. and Godfraind, T. (1981) Biochim. Biophys. Acta 649, 651–660
19 Wuytack, F., Landon, E., Fleischer, S. and Hardman, J.P. (1978) Biochim. Biophys. Acta 540, 253–269
20 Wuytack, F. and Casteels, R. (1980) Biochim. Biophys. Acta 595, 257–263
21 Grover, A.K. and Kwan, C.Y. (1983) Life Sci. 32, 2655–2660
22 Grover, A.K., Frederickson, M. and Daniel, E.E. (1981) Can. J. Physiol. Pharmacol. 59, 1180–1183